Nanoscale Advances

ROYAL SOCIETY OF CHEMISTRY

PAPER

View Article Online
View Journal | View Issue

Cite this: *Nanoscale Adv.*, 2022, **4**, 2922

Superprotonic conduction of intrinsically zwitterionic microporous polymers based on easy-to-make squaraine, croconaine and rhodizaine dyes†

Dominic Taylor,‡[b] Xuanhe Hu,‡[a] Can-Min Wu,[b] John M. Tobin,‡[b] Zuzana Oriou,[c] Jun He,*[a] Zhengtao Xu*[d] and Filipe Vilela*[b]

Received 23rd March 2022
Accepted 7th June 2022

DOI: 10.1039/d2na00177b

rsc.li/nanoscale-advances

Porous organic polymers (POPs) have been prepared *via* a novel metal free polycondensation between a tritopic indole-based monomer and squaric, croconic and rhodizonic acids. Each of the three POPs exhibited high BET surface areas (331–667 m^2 g^{-1}) and zwitterionic structures. Impedance measurements revealed that the intrinsic POPs were relatively weak proton conductors, with a positive correlation between the density of oxo-groups and the proton conduction. Doping the materials with LiCl vastly improved the proton conductivity up to a value of 0.54 S cm^{-1} at 90 °C and 90% relative humidity.

Introduction

Ionic conduction, vital for energy technologies such as fuel cells and batteries, remains a challenging property to optimize in the solid state, as the mobility of protons and other ions depends on many structural and environmental factors.[1–4] Of general importance is the number of charge carriers, *e.g.*, in the form of built-in $-SO_3H$ or other ionic/acidic groups, and of ionic guests and water molecules introduced into the channels of the porous host. These charge carriers should have freedom to undergo dynamic motion and should exhibit relatively weak interactions with the host framework. Furthermore, they should be optimally spaced and orientated for passing along the H^+, Li^+ or other mobile ions.[5] It is therefore a delicate balancing act to modify the structure and functions for achieving higher ionic conductivity.

In this context, metal–organic frameworks (MOF),[6] and porous organic polymers (POP),[7–9] offer structural and functional modifiability (largely from the highly variable organic building blocks),[10,11] and therefore great opportunity to explore and improve solid state ionic conduction properties.[1,3,4] Incidentally, POP frameworks offer the advantage of stability, especially to the aqueous acidic/basic conditions common in fuel cell setups as compared with many hydrolytically labile MOFs. Equipping the framework backbones with sulfonic and other acidic groups is a tried-and-true method, as dense arrays of appended $-SO_3H$ groups can help reach record level of proton conductivity.[12–14] Many other functions have been also tried to improve ionic conductivity, including phosphonic acid,[15] Troger's base (for anion exchange membranes),[16] and heterocyclic guests such as 1*H*-imidazole or 1*H*-1,2,3-triazole (*e.g.* for the non-diffusive relay-like proton transport pathway).[17]

On the other hand, doping ionic guests such as LiCl into the host matrix offers a potentially versatile approach to improving ionic conductivity, because of the diverse array of ionic guests that can be post-synthetically inserted for optimization studies.[18–20] For this, a host material exhibiting strong ionic character in the form of a zwitterionic POP will facilitate uptake of the ionic dopants of inorganic salts. Such salts are hydrophilic and well-hydrated species will be reluctant to penetrate the typically less polar organic matrix of POPs. Zwitterionic POPs remain, however, surprisingly rare. For example, the commonly used amine-carbonyl condensations using 1,3,5-triformylphloroglucinol do not generate polymer frameworks with sufficient ionic character, and extra base/acid groups have to be appended to impart distinct zwitterionic properties.[21–26] Although zwitterionic POPs have recently started to be explored as ionic conduction materials, studies on inserting ionic salt (*e.g.*, LiCl) dopants for boosting conductivity remains unknown for zwitterionic POP systems.

Reported here is an efficient synthesis of a series of zwitterionic POPs that can be LiCl-doped (by soaking in a saturated

[a]*School of Chemical Engineering and Light Industry, Guangdong University of Technology, Guangzhou, Guangdong 510006, China. E-mail: junhe@gdut.edu.cn*

[b]*School of Engineering and Physical Sciences, Heriot-Watt University, Edinburgh, EH14 4AS, UK. E-mail: f.vilela@hw.ac.uk*

[c]*Materials Innovation Factory and Department of Chemistry, University of Liverpool, Crown Street, Liverpool, L69 7ZD, UK*

[d]*Institute of Materials Research and Engineering, 2 Fusionopolis Way, Innovis Building, Singapore 138634. E-mail: zhengtao@imre.a-star.edu.sg*

† Electronic supplementary information (ESI) available: Synthesis and characterisation of compound **1** and polymers **PSQ**, **PCR** and **PRH**. See https://doi.org/10.1039/d2na00177b

‡ These authors contributed equally.

THF solution) to achieve proton conductivity as high as 0.54 S cm^{-1} at 90 °C and 90% relative humidity. The distinct zwitterionic character of the polymer framework stems from the condensation between indole and the oxocarbon anions of squaric (**SQ**), croconic (**CR**) and rhodozonic (**RH**) acids. **SQ** and **CR** in particular have shown importance as precursors to near-infrared (NIR) absorbing dyes and their ability to undergo condensation reactions with indole, pyrrole or aniline derivatives can generate a plethora of possible structures.[27] This includes examples of POPs featuring squaraine groups spanning applications such as photocatalysis and energy storage.[28–30] However, to our knowledge **CR** and **RH** have not yet been successfully incorporated into POPs. Our key hypothesis here is that the larger **CR** and **RH**, with higher density of the polar oxo-groups, may facilitate the uptake of the ionic guests and enhance proton transport throughout the polymer matrix.

Results and discussion

Polymer synthesis and characterization

For constructing the polymer framework, the tritopic indole-based monomer (**1**) was prepared *via* the Suzuki–Miyaura cross-coupling between 1,3,5-benzenetriboronic acid pinacol ester and 2,3,3-trimethyl-5-bromo-3*H*-indole (Scheme 1). Subsequent polycondensation of **1** with **SQ**, **CR** and **RH** acids yielded three novel POP materials (Scheme 2). **SQ**, along with the lesser investigated **CR** and **RH** acids, are known to undergo condensation reactions with electron-rich aromatic molecules including pyrrole, indole or aniline derivatives, with water being the condensation by-product.[27] This approach has been implemented to yield a variety of conjugated poly(squaraines), showing a modulation in the bandgap as well as a bathochromic shift in absorbance values.[31] Therefore, we employed the electron-rich indole **1** in three metal-free polycondensation reactions utilizing **SQ**, **CR** and **RH** acids to synthesize three POPs (**PSQ**, **PCR** and **PRH** respectively), each with an alternating acid–indole polymeric network. The reactions were performed with quinoline in a butanol/toluene (1 : 1) solvent mixture under a nitrogen atmosphere at 120 °C for 72 h (Scheme 2). After cooling, the precipitate was filtered, washed and purified *via* Soxhlet extraction with toluene, chloroform and methanol then subsequently dried *in vacuo*. The POPs were isolated with excellent recoveries in the range of 85–97%. In short, we were thus able to integrate **SQ**, **CR** and **RH** dyes into a POP structure, without using metal catalysts in the polymerization step.[32–41]

The resulting POPs were characterized *via* spectroscopic methods and other analytical methods were employed to determine their physical characteristics. Analysis of FTIR spectroscopy proved difficult to determine formation of the polymers. However, a sharp band at ~2960 cm^{-1} in **1** indicates the presence of methyl groups found on the indole (Fig. S2†). This peak, while still present, reduces significantly in the spectra of the POPs, indicating the formation of a bond between the lone methyl group and the acid. Solid state ^{13}C NMR analysis was also employed as a further spectroscopic method to determine the functional groups within the POPs. Each group in the **PSQ** and **PCR** spectra was well defined. A detailed assignment of the spectra peaks can be found in the ESI (Fig. S4–S6†). However, **PRH** showed some anomalies when compared to the **PSQ** and **PCR** spectra. The most notable difference was the near disappearance of the signals around 180 ppm which are indicative of a ketone functional group that can be found in **RH**. A new peak at 67 ppm also arises though this can be explained as a shift in the C–OH (O^-) peak as it falls within the standard range of this functional group.

UV-Vis spectroscopy of the POPs (Fig. 1) show a large bathochromic shift into the visible red and near IR region of the spectrum. While **PSQ** possesses an absorption maxima (λ_{max}) located at 700 nm, both **PCR** and **PRH** have λ_{max} located at approximately 800 nm. Interestingly, although **PCR** and **PRH** display similar absorbance maxima, the spectra are somewhat dissimilar. **PCR** exhibits a very broad absorption beginning at 1050 nm and dipping at 630 nm. However, **PRH** shows only a small local maximum at ~800 nm which is relatively weak compared to the absorbance between 400-600 nm.

The thermal stability of the POPs was assessed using thermogravimetric analysis (TGA, Fig. S9–S11†) in the temperature region of 25–950 °C under a flow of CO_2 using an empty alumina crucible as the reference sample. The POPs exhibited a slight change in mass when heating to 100 °C: this could be due to residual solvent trapped in the pores. Decomposition of the POPs began in the region of 150–200 °C and continued until 550 °C, at which point less than 10% of the initial mass was remaining. In comparison to other POPs, those reported here exhibited low thermal stability. This could suggest that the connection formed *via* the polycondensation is susceptible to thermal cleavage.

The surface area of the three POPs was measured *via* N_2 and CO_2 gas adsorption experiments at 77 K and 273 K respectively (Table 1, Fig. S12–S23†). The CO_2 adsorption measurements

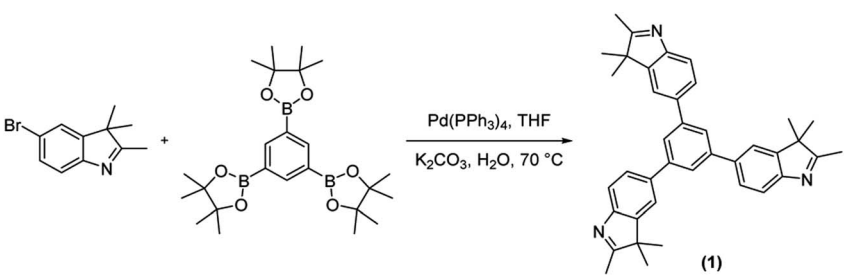

Scheme 1 Synthesis of tritopic indole linker through Suzuki–Miyaura cross-coupling.

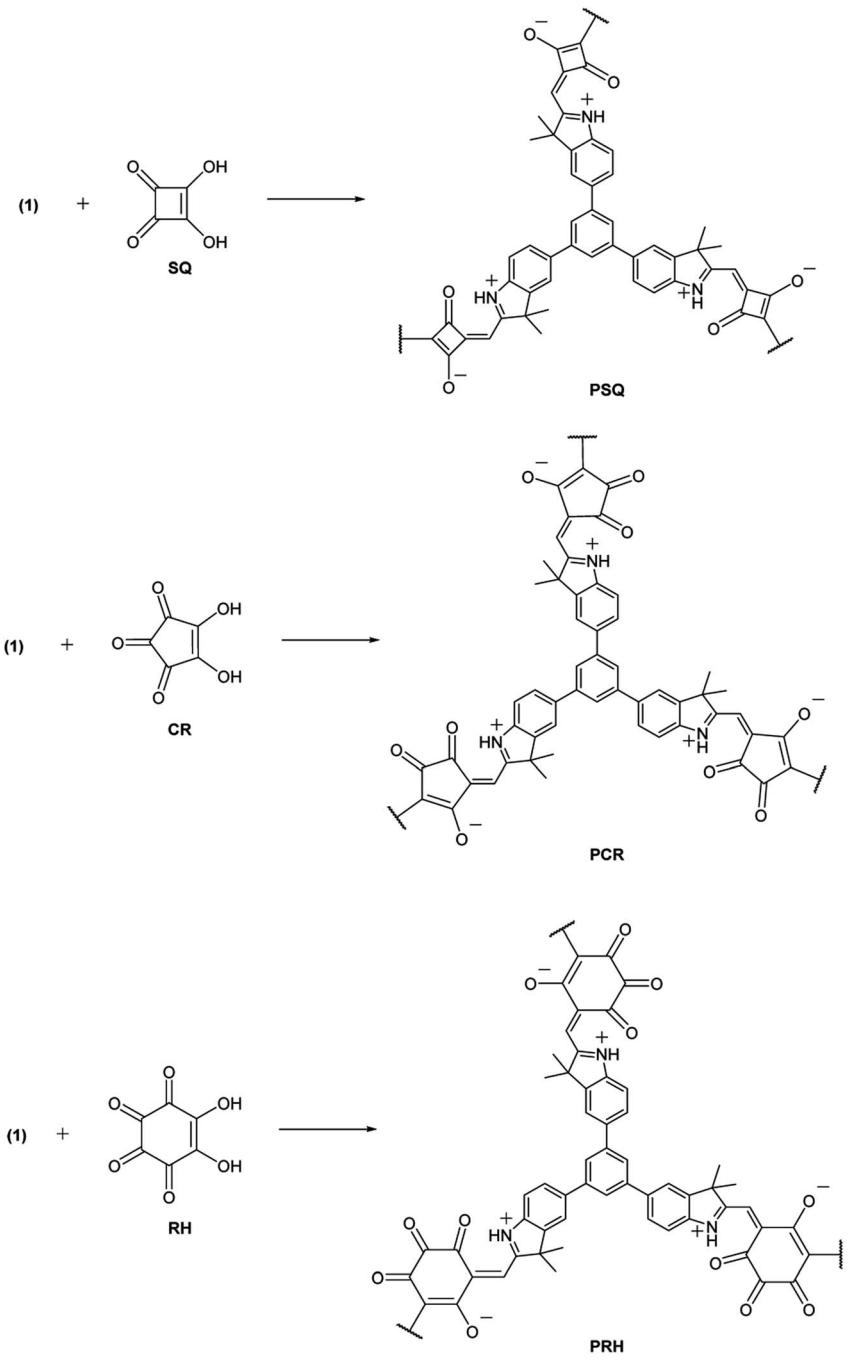

Scheme 2 Synthesis of three POPs through polycondensation of **1** with **SQ**, **CR** and **RH**. Reaction conditions: quinoline (6 mol%), butanol/toluene (v/v 1 : 1), 72 h, Dean–Stark apparatus with 3 Å molecular sieves.

revealed that the three materials exhibited high BET surface areas (385–472 $m^2\ g^{-1}$) although utilizing N_2 as the probe molecule led to much lower surface areas (2.3–106 $m^2\ g^{-1}$). This discrepancy most likely stems from the use of N_2 at cryogenic temperatures, which has been reported to kinetically restrict access to smaller micropores.[42–44] By comparison, the use of CO_2 as the probe molecule utilizes higher temperatures and pressures, allowing for faster diffusion and analysis of smaller micropores. For each of the POPs, type 1 CO_2 adsorption isotherms were observed, which is typical for microporous polymers. The pore size distribution and pore volumes were modelled using the QSDFT (N_2 isotherms) and the Monte-Carlo models (CO_2 isotherms), revealing the presence of mainly micropores with additional mesopores.[45] The pore volumes that were measured by N_2 gas sorption were particularly low (0.005–0.09 $cm^3\ g^{-1}$), although the range of values obtained through CO_2 gas sorption experiments (0.131–0.220 $cm^3\ g^{-1}$) were more in line with values expected for POPs. The origin of this could potentially be due to inability of the N_2 probe gas to fully access the microporous structures of the three POPs, thus

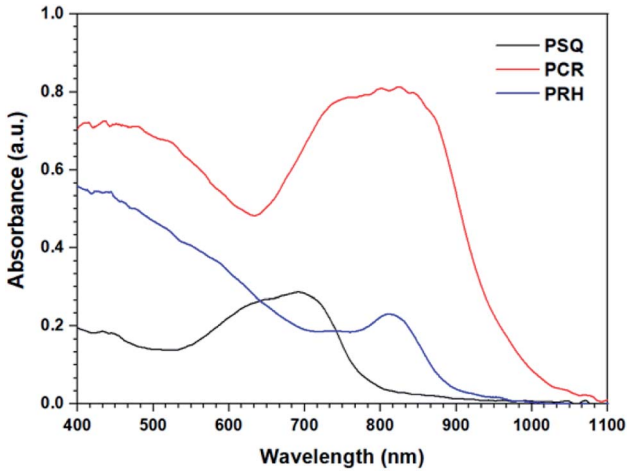

Fig. 1 UV-Vis spectra of **PSQ**, **PCR** and **PRH** with local λ_{max} ranging from 700–850 nm.

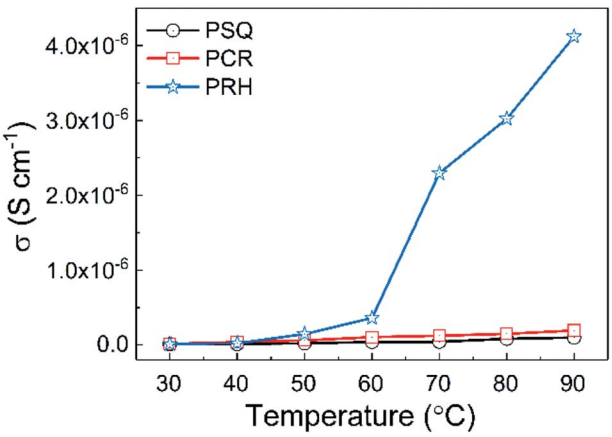

Fig. 2 Proton conductivity of **PSQ**, **PCR**, **PRH** at different temperatures (from 30 °C to 90 °C) and 90% relative humidity.

Table 1 Summary of the surface area and porous features of the synthesised POPs

Material	S_{BET}/m^2 g^{-1}	Average pore width/nm	Pore volume/cm^3 g^{-1}
PSQ	106[a]	2.382	0.09
	385[b]	0.822	0.220
PCR	2.3[a]	3.096	0.005
	405[b]	0.458	0.131
PRH	42[a]	2.6	0.056
	472[b]	0.785	0.172

[a] Measured using N_2 gas at 77 K. [b] Measured using CO_2 gas at 273 K.

underestimating the pore volume significantly. The morphology of **PSQ**, **PCR** and **PRH** were all analyzed *via* scanning electron microscopy (SEM), revealing textured surfaces (Fig. S24–S26†). **PCR** and **PRH** both exhibited globular morphologies while **PSQ** was less well defined in its texture.

Proton conductivity measurements

The proton conductivities of pristine POPs were first measured by impedance spectrometry from 30 to 90 °C under 90% relative humidity (Fig. 2, S27 and S28†). It turned out that **PSQ**, **PCR** and **PRH** exhibits relatively low conductivities in the range of 0.98 to 41 × 10^{-7} S cm^{-1} at 90 °C and 90% relative humidity. All of the POPs displayed an increase in conductivity with increasing temperature, which can be attributed to the enhanced diffusivity and ionic mobility at elevated temperature.[46] Moreover, the proton conductivities at temperatures above 50 °C follow the order **PSQ** < **PCR** < **PRH**, indicating that POPs with a higher density of the polar oxo-groups may facilitate binding of hydrated proton by hydrogen-bonding and thus promote proton transport throughout the polymer matrix.[47–49]

Considering that **SQ** and **CR** have shown importance as precursors to NIR dyes, the effect of illumination on proton conductivities of POPs was explored. The proton conductivities of the three POPs were then measured after being illuminated by a red LED for different times at 90 °C and 90% relative humidity (Fig. S29 and S30†). However, our results show that illumination has a negligible and negative association with the proton conductivity. As the proton conductivities of the intrinsic POPs were all relatively low, we sought to increase the proton conductivities by doping the material with charge carriers. This is a method that has been previously explored with other proton conductive materials using ionic salts (*e.g.*, LiCl, Cs_2CO_3),[18,20] or electrolytes (*e.g.* imidazole, triazole).[19,50] With this in mind, we doped **PSQ**, **PCR** and **PRH** with LiCl by soaking the POPs in LiCl/THF for 2 days at room temperature (Fig. S31–S36, see ESI for synthetic details†). This led to six orders of magnitude improvement in the proton conductivity, with values in the range of 0.88 to 5.4 × 10^{-1} S cm^{-1} at 90 °C and 90% relative humidity, which are comparable to the conventional Nafion (0.08 S cm^{-1}, Fig. 3, Table S1†).[18] According to previous studies, this huge increase in the conductivity may have be achieved by facilitating Li^+ ion movements in the POPs. It is worth noting that after introducing LiCl, the proton conductivities kept the order **PSQ** < **PCR** < **PRH**, further confirming POPs rich in oxo-groups can boost proton transport. As

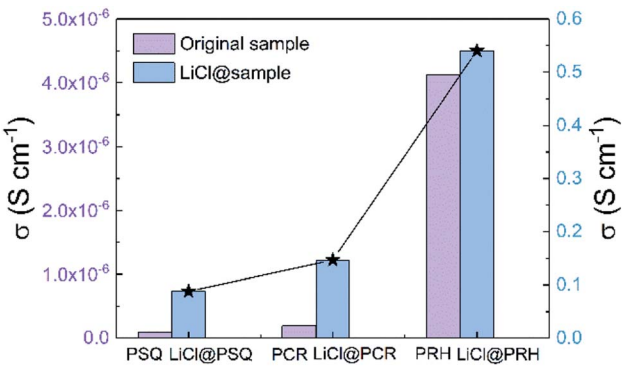

Fig. 3 Proton conductivity of **PSQ**, **PCR**, **PRH** and **LiCl@PSQ**, **LiCl@PCR**, **LiCl@PRH** at 90 °C and 90% relative humidity.

a result, the greatest proton conductivity of 5.4×10^{-1} S cm^{-1} for **LiCl@PRH** was obtained at 90 °C and 90% relative humidity.[51] In addition, the activation energy (E_a) of the proton conduction in three POPs were estimated from Arrhenius plots to be 0.26–0.40 eV (Fig. S30c–S35c†). Such E_a values are typical for the Grotthuss mechanism (E_a < 0.4 eV), which involves proton hopping between adjacent media accompanied by rotational reorientation motion.[52–55]

Conclusions

In conclusion, a novel method to prepare POPs *via* the metal free polycondensation between a tritopic indole-based linker and squaric, croconic and rhodizonic acids has been developed. Impedance measurements carried out on the pristine polymer materials revealed that they were relatively weak proton conductors. A positive correlation between the proton conductivities at high temperature and the density of oxo-groups in the POPs was observed, suggesting that these groups facilitate proton binding through hydrogen bonding. Doping these materials with LiCl led to vastly improved proton conduction up to 5.4×10^{-1} S cm^{-1} at 90 °C and 90% relative humidity.

Funding sources

This work was partially funded by the National Natural Science Foundation of China (21871061) and Science and Technology Planning Project of Guangdong Province (2021A0505030066). DT and FV acknowledge the EPSRC funded (EP/L016419/1) CRITICAT Centre for Doctoral Training for Dominic Taylor's PhD. ZX acknowledges a GRF grant from the Research Grants Council of HKSAR (CityU 11303519).

Author contributions

The manuscript was written through contributions of all authors. All authors have given approval to the final version of the manuscript.

Conflicts of interest

The authors declare no competing financial interest.

Acknowledgements

We thank Hua-Qun Zhou and Dr Yonghe He for their help with this work.

References

1 X. Zhao, Y. Chen, Z. Wang and Z. Zhang, Design and Application of Covalent Organic Frameworks for Ionic Conduction, *Polym. Chem.*, 2021, **12**(34), 4874–4894.
2 A. Gupta, S. Goswami, S. M. Elahi and S. Konar, Role of Framework-Carrier Interactions in Proton-Conducting Crystalline Porous Materials, *Cryst. Growth Des.*, 2021, **21**(3), 1378–1388.
3 D. W. Lim and H. Kitagawa, Proton Transport in Metal-Organic Frameworks, *Chem. Rev.*, 2020, **120**(16), 8416–8467.
4 D. W. Kang, M. Kang and C. S. Hong, Post-Synthetic Modification of Porous Materials: Superprotonic Conductivities and Membrane Applications in Fuel Cells, *J. Mater. Chem. A*, 2020, **8**(16), 7474–7494.
5 S. Kim, B. Joarder, J. A. Hurd, J. Zhang, K. W. Dawson, B. S. Gelfand, N. E. Wong and G. K. H. Shimizu, Achieving Superprotonic Conduction in Metal-Organic Frameworks through Iterative Design Advances, *J. Am. Chem. Soc.*, 2018, **140**(3), 1077–1082.
6 S. Yuan, L. Feng, K. Wang, J. Pang, M. Bosch, C. Lollar, Y. Sun, J. Qin, X. Yang, P. Zhang, *et al.*, Stable Metal–Organic Frameworks: Design, Synthesis, and Applications, *Adv. Mater.*, 2018, **30**(37), 1–35.
7 N. B. McKeown and P. M. Budd, Polymers of Intrinsic Microporosity (PIMs): Organic Materials for Membrane Separations, Heterogeneous Catalysis and Hydrogen Storage, *Chem. Soc. Rev.*, 2006, **35**(8), 675–683.
8 T. Ben and S. Qiu, Porous Aromatic Frameworks: Synthesis, Structure and Functions, *CrystEngComm*, 2013, **15**(1), 17–26.
9 Y. Yuan and G. Zhu, Porous Aromatic Frameworks as a Platform for Multifunctional Applications, *ACS Cent. Sci.*, 2019, **5**(3), 409–418.
10 D. Taylor, S. J. Dalgarno, Z. Xu and F. Vilela, Conjugated Porous Polymers: Incredibly Versatile Materials with Far-Reaching Applications, *Chem. Soc. Rev.*, 2020, **49**(12), 3981–4042.
11 D. Taylor, S. J. Dalgarno and F. Vilela, Structure–Function Relationship in Conjugated Porous Polymers, in *Concepts and Design of Materials Nanoarchitectonics*, 2022, pp. 226–246.
12 S. Mukhopadhyay, J. Debgupta, C. Singh, R. Sarkar, O. Basu and S. K. Das, Designing UiO-66-Based Superprotonic Conductor with the Highest Metal-Organic Framework Based Proton Conductivity, *ACS Appl. Mater. Interfaces*, 2019, **11**(14), 13423–13432.
13 F. Yang, G. Xu, Y. Dou, B. Wang, H. Zhang, H. Wu, W. Zhou, J. R. Li and B. Chen, A Flexible Metal-Organic Framework with a High Density of Sulfonic Acid Sites for Proton Conduction, *Nat. Energy*, 2017, **2**(11), 877–883.
14 Y. He, J. Dong, Z. Liu, M. Q. Li, J. Hu, Y. Zhou, Z. Xu and J. He, Dense Dithiolene Units on Metal-Organic Frameworks for Mercury Removal and Superprotonic Conduction, *ACS Appl. Mater. Interfaces*, 2022, **14**(1), 1070–1076.
15 J. M. Taylor, K. W. Dawson and G. K. H. Shimizu, A Water-Stable Metal-Organic Framework with Highly Acidic Pores for Proton-Conducting Applications, *J. Am. Chem. Soc.*, 2013, **135**(4), 1193–1196.
16 X. Du, Y. Yuan, T. Dong, X. Chi and Z. Wang, Polymer Electrolyte Membranes from Microporous Troger's Base Polymers for Fuel Cells, *ACS Appl. Energy Mater.*, 2021, **4**(11), 13327–13334.
17 D. Basak, C. Versek, J. A. Harvey, S. Christensen, J. Hillen, S. M. Auerbach, M. T. Tuominen and D. Venkataraman, Enhanced Anhydrous Proton Conduction in Binary

Mixtures of 1*H*-Imidazole-1*H*-1,2,3-Triazole Based Compounds, *J. Mater. Chem.*, 2012, **22**(38), 20410–20417.

18 S. Horike, Y. Kamitsubo, M. Inukai, T. Fukushima, D. Umeyama, T. Itakura and S. Kitagawa, Postsynthesis Modification of a Porous Coordination Polymer by LiCl to Enhance H^+ Transport, *J. Am. Chem. Soc.*, 2013, **135**(12), 4612–4615.

19 S. Nandi, V. M. Dhavale, S. Shalini, U. Werner-Zwanziger, H. Singh, S. Kurungot and R. Vaidhyanathan, Lithium-Assisted Proton Conduction at 150 °C in a Microporous Triazine-Phenol Polymer, *Adv. Mater. Interfaces*, 2015, **2**(16), 1–7.

20 S. Shalini, S. Aggarwal, S. K. Singh, M. Dutt, T. G. Ajithkumar and R. Vaidhyanathan, 10000-Fold Enhancement in Proton Conduction by Doping of Cesium Ions in a Proton-Conducting Zwitterionic Metal–Organic Framework, *Eur. J. Inorg. Chem.*, 2016, **2016**(27), 4382–4386.

21 Y. Yang, W. Zhao, H. Niu and Y. Cai, Mechanochemical Construction 2D/2D Covalent Organic Nanosheets Heterojunctions Based on Substoichiometric Covalent Organic Frameworks, *ACS Appl. Mater. Interfaces*, 2021, **13**(35), 42035–42043.

22 S. Chandra, T. Kundu, K. Dey, M. Addicoat, T. Heine and R. Banerjee, Interplaying Intrinsic and Extrinsic Proton Conductivities in Covalent Organic Frameworks, *Chem. Mater.*, 2016, **28**(5), 1489–1494.

23 S. Kandambeth, A. Mallick, B. Lukose, M. V. Mane, T. Heine and R. Banerjee, Construction of Crystalline 2D Covalent Organic Frameworks with Remarkable Chemical (Acid/Base) Stability *via* a Combined Reversible and Irreversible Route, *J. Am. Chem. Soc.*, 2012, **134**(48), 19524–19527.

24 Z. J. Mu, X. Ding, Z. Y. Chen and B. H. Han, Zwitterionic Covalent Organic Frameworks as Catalysts for Hierarchical Reduction of CO_2 with Amine and Hydrosilane, *ACS Appl. Mater. Interfaces*, 2018, **10**(48), 41350–41358.

25 Y. Li, H. Wu, Y. Yin, L. Cao, X. He, B. Shi, J. Li, M. Xu and Z. Jiang, Fabrication of Nafion/Zwitterion-Functionalized Covalent Organic Framework Composite Membranes with Improved Proton Conductivity, *J. Membr. Sci.*, 2018, **568**, 1–9.

26 Y. Fu, Y. Wu, S. Chen, W. Zhang, Y. Zhang, T. Yan, B. Yang and H. Ma, Zwitterionic Covalent Organic Frameworks: Attractive Porous Host for Gas Separation and Anhydrous Proton Conduction, *ACS Nano*, 2021, **15**(12), 19743–19755.

27 L. Beverina and P. Salice, Squaraine Compounds: Tailored Design and Synthesis towards a Variety of Material Science Applications, *Eur. J. Org. Chem.*, 2010, **7**, 1207–1225.

28 A. Nagai, X. Chen, X. Feng, X. Ding, Z. Guo and D. Jiang, A Squaraine-Linked Mesoporous Covalent Organic Framework, *Angew. Chem., Int. Ed.*, 2013, **52**(13), 3770–3774.

29 R. Xue, H. Gou, L. Zhang, Y. Liu, H. Rao and G. Zhao, A New Squaraine-Triazine Based Covalent Organic Polymer as an Electrode Material with Long Life and High Performance for Supercapacitors, *New J. Chem.*, 2021, **45**(2), 679–684.

30 X. Zhang, J. Zhao, Y. Zhao, Z. Bakenov and Y. Zhang, Engineering Zwitterionic Barrier by Squaraine-Based Porous Organic Framework Fiber for Superior Lithium-Sulfur Batteries, *Electrochim. Acta*, 2021, **397**, 139276.

31 A. Ajayaghosh, Donor-Acceptor Type Low Band Gap Polymers: Polysquaraines and Related Systems, *Chem. Soc. Rev.*, 2003, **32**(4), 181–191.

32 X. Ding and B. H. Han, Copper Phthalocyanine-Based CMPs with Various Internal Structures and Functionalities, *Chem. Commun.*, 2015, **51**(64), 12783–12786.

33 J. Lee, O. Buyukcakir, T. W. Kwon and A. Coskun, Energy Band-Gap Engineering of Conjugated Microporous Polymers *via* Acidity-Dependent *In situ* Cyclization, *J. Am. Chem. Soc.*, 2018, **140**(35), 10937–10940.

34 M. Liu, C. Yao, C. Liu and Y. Xu, Ag^+ Doped into Azo-Linked Conjugated Microporous Polymer for Volatile Iodine Capture and Detection of Heavy Metal Ions, *Sci. Rep.*, 2018, **8**(1), 14072.

35 Y. Kou, Y. Xu, Z. Guo and D. Jiang, Supercapacitive Energy Storage and Electric Power Supply Using an Aza-Fused π-Conjugated Microporous Framework, *Angew. Chem., Int. Ed.*, 2011, **50**(37), 8753–8757.

36 Y. Wei, W. Chen, X. Zhao, S. Ding, S. Han and L. Chen, Solid-State Emissive Cyanostilbene Based Conjugated Microporous Polymers: *Via* Cost-Effective Knoevenagel Polycondensation, *Polym. Chem.*, 2016, **7**(24), 3983–3988.

37 Z. H. Guo, C. Wang, Q. Zhang, S. Che, H. C. Zhou and L. Fang, Cost-Effective Synthesis and Solution Processing of Porous Polymer Networks through Methanesulfonic Acid-Mediated Aldol Triple Condensation, *Mater. Chem. Front.*, 2018, **2**(2), 396–401.

38 P. Ju, S. Wu, Q. Su, X. Li, Z. Liu, G. Li and Q. Wu, Salen-Porphyrin-Based Conjugated Microporous Polymer Supported Pd Nanoparticles: Highly Efficient Heterogeneous Catalysts for Aqueous C–C Coupling Reactions, *J. Mater. Chem. A*, 2019, **7**(6), 2660–2666.

39 Z. Li, X. Li and Y. W. Yang, Conjugated Macrocycle Polymer Nanoparticles with Alternating Pillarenes and Porphyrins as Struts and Cyclic Nodes, *Small*, 2019, **15**(12), 1–10.

40 B. P. Biswal, D. Becker, N. Chandrasekhar, J. S. Seenath, S. Paasch, S. Machill, F. Hennersdorf, E. Brunner, J. J. Weigand, R. Berger, et al. Exploration of Thiazolo[5,4-*d*]Thiazole Linkages in Conjugated Porous Organic Polymers for Chemoselective Molecular Sieving, *Chem.–Eur. J.*, 2018, **24**(42), 10868–10875.

41 Q. Huang, L. Guo, N. Wang, X. Zhu, S. Jin and B. Tan, Layered Thiazolo[5,4- *d*] Thiazole-Linked Conjugated Microporous Polymers with Heteroatom Adoption for Efficient Photocatalysis Application, *ACS Appl. Mater. Interfaces*, 2019, **11**(17), 15861–15868.

42 J. Weber, J. Schmidt, A. Thomas and W. Böhlmann, Micropore Analysis of Polymer Networks by Gas Sorption and 129Xe NMR Spectroscopy: Toward a Better Understanding of Intrinsic Microporosity, *Langmuir*, 2010, **26**(19), 15650–15656.

43 D. Lozano-Castelló, D. Cazorla-Amorós and A. Linares-Solano, Usefulness of CO_2 Adsorption at 273 K for the Characterization of Porous Carbons, *Carbon*, 2004, **42**(7), 1233–1242.

44 K. A. Cychosz and M. Thommes, Progress in the Physisorption Characterization of Nanoporous Gas Storage Materials, *Engineering*, 2018, **4**(4), 559–566.

45 J. Rouquerol, D. Avnir, C. W. Fairbridge, D. H. Everett, J. M. Haynes, N. Pernicone, J. D. F. Ramsay, K. S. W. Sing and K. K. Unger, Recommendations for the Characterization of Porous Solids, *Pure Appl. Chem.*, 1994, **66**(8), 1739–1758.

46 L. Liu, W. Chen and Y. Li, An Overview of the Proton Conductivity of Nafion Membranes through a Statistical Analysis, *J. Membr. Sci.*, 2016, **504**, 1–9.

47 S. K. Konavarapu, A. Goswami, A. G. Kumar, S. Banerjee and K. Biradha, MOFs Containing a Linear Bis-Pyridyl-Tris-Amide and Angular Carboxylates: Exploration of Proton Conductivity, Water Vapor and Dye Sorptions, *Inorg. Chem. Front.*, 2019, **6**(1), 184–191.

48 T. Kawabata and Y. Matsuo, Role of Acetyl Group on Proton Conductivity in Chitin System, *J. Mater.*, 2019, **5**(2), 258–263.

49 S. S. Xue, X. X. Li, Y. M. Lee, M. S. Seo, Y. Kim, S. Yanagisawa, M. Kubo, Y. K. Jeon, W. S. Kim, R. Sarangi, *et al.*, Enhanced Redox Reactivity of a Nonheme Iron(V)-Oxo Complex Binding Proton, *J. Am. Chem. Soc.*, 2020, **142**(36), 15305–15319.

50 Y. Ye, L. Zhang, Q. Peng, G. E. Wang, Y. Shen, Z. Li, L. Wang, X. Ma, Q. H. Chen, Z. Zhang, *et al.*, High Anhydrous Proton Conductivity of Imidazole-Loaded Mesoporous Polyimides over a Wide Range from Subzero to Moderate Temperature, *J. Am. Chem. Soc.*, 2015, **137**(2), 913–918.

51 S. Li, Y. Zhao, S. Knoll, R. Liu, G. Li, Q. Peng, P. Qiu, D. He, C. Streb and X. Chen, High Proton-Conductivity in Covalently Linked Polyoxometalate Organoboronic Acid-Polymers, *Angew. Chem., Int. Ed.*, 2021, **60**(31), 16953–16957.

52 S. Pili, S. P. Argent, C. G. Morris, P. Rought, V. García-Sakai, I. P. Silverwood, T. L. Easun, M. Li, M. R. Warren, C. A. Murray, *et al.*, Proton Conduction in a Phosphonate-Based Metal-Organic Framework Mediated by Intrinsic "Free Diffusion inside a Sphere", *J. Am. Chem. Soc.*, 2016, **138**(20), 6352–6355.

53 Y. Wang, J. Yin, D. Liu, C. Gao, Z. Kang, R. Wang, D. Sun and J. Jiang, Guest-tuned proton conductivity of a porphyrinylphosphonate-based hydrogenbonded organic framework, *J. Mater. Chem. A*, 2021, **9**(5), 2683–2688.

54 X. Jiang, K. Zhang, Y. Huang, B. Xu, X. Xu, J. Zhang, Z. Liu, Y. Wang, Y. Pan, S. Bian, *et al.*, Conjugated Microporous Polymer with C≡C and C–F Bonds: Achieving Remarkable Stability and Super Anhydrous Proton Conductivity, *ACS Appl. Mater. Interfaces*, 2021, **13**(13), 15536–15541.

55 L. Xin, D. Zhang, K. Qu, Y. Lu, Y. Wang, K. Huang, Z. Wang, W. Jin, Z. Xu, *et al.*, Zr-MOF-Enabled Controllable Ion Sieving and Proton Conductivity in Flow Battery Membrane, *Adv. Funct. Mater.*, 2021, **31**(42), 2104629.